Toroidal Plasma Rotation in the PLT Tokamak with Neutral-Beam Injection

S. Suckewer, H. P. Eubank, R. J. Goldston,

J. McEnerney, N. R. Sauthoff, and H. H. Towner

Plasma Physics Laboratory, Princeton University

Princeton, New Jersey

ABSTRACT

Toroidal plasma rotation in the Princeton Large Torus, PLT, has been measured for various plasma and neutral beam injection conditions. Measurements of the plasma rotational velocities were made from Doppler shifts of appropriate spectral lines and include data from both hydrogen and deuterium beams and co- and counter-injection at several electron densities. Without injection, a small but consistent toroidal rotation exists in a direction opposite to the plasma current (counter-direction) in the plasma center but parallel to the current (co-direction) in the plasma periphery. Using these measured velocities and the plasma density and temperature gradients, radial electron fields can be determined from theory, giving $E_r \approx 40$ V/cm near the plasma center and $E_r \approx 10$ V/cm near the plasma edge. Insertion of a local, 2.5 percent magnetic well produced no observable effect on the beam driven rotation. Modeling of the time evolution and radial distribution of the rotation allows one to deduce an effective viscosity of the order of (1-5) x 10^4 cm^2/sec.

I. INTRODUCTION

Toroidal plasma rotation induced by the momentum input associated with unbalanced neutral beam injection is of considerable interest since it complements the analyses of mass and energy confinement, yielding further insight into the basis of tokamak transport processes. The assumption of axisymmetry, so fundamental to neoclassical transport theory, is clearly violated by rapid braking of toroidal rotation. In addition, while many tokamak neutral beam injection systems are designed to impart very little net momentum, either by virtue of an aiming angle almost perpendicular to the magnetic field or by canceling the momentum through equal numbers of injectors aimed parallel (co) and antiparallel (counter) to the plasma current, there are some potential advantages which accrue from unbalanced tangential co-injection. The extent to which unbalanced injection systems can be employed without incurring detrimental side effects upon energy confinement from the concomitant rotation and the means by which selective momentum damping processes may be used to control plasma rotation are of great concern to the tokamak community.

Recent experiments with neutral beam injection (NBI) into the Impurity Studies Experiment (ISX) [1] and PLT [2] tokamaks have shown that with co-injection the influx of medium- and high- Z impurities is much lower than in the case of counter-injection. The extent to which these observations can be explained by different impurity source terms, due to the poorer confinement properties of counter-injection beams, different temperature profiles, electric fields induced by rotation, or to the effect of proposed beam driven impurity flow [3,4] is the subject of extensive current research efforts. One would likely take advantage of the experimental observations, whatever the explanation, in the design of new larger tokamaks such as the Tokamak Fusion

Test Reactor, TFTR, were it not for concern over possible instabilities associated with toroidal plasma rotation at near thermal speeds.

The PLT experiments reported here were made in an effort to address many of the above questions. To this purpose, we have used both hydrogen and deuterium beams over a range of input powers up to ~ 1 MW and have studied rotation for a range of electron densities. In addition, the influence of toroidal field ripple [5,6] initially introduced by minor damage to a toroidal field coil and later in a controlled fashion by a coil shunt, has been studied in the light of its possible damping effect.

II. EXPERIMENTAL RESULTS

Toroidal plasma velocity was measured from the Doppler shift of ion spectral lines with the techniques described earlier [7,8]. For central plasma velocities ($5 \leq r \leq 10$ cm) an optically forbidden line of highly ionized iron (FeXX 2665Å) was used, while at the plasma periphery ($27 \leq r \leq 33$ cm) a carbon line (CV 2271Å) was used. Radial distributions of the ions FeXX and CV were measured from radial line intensity profiles. For most experiments, the plasma current was in the range 400-450 kA but some measurements were made with currents as low as 300 kA. Limiter (carbon or steel) positions were at a radius of 40 cm. Central electron temperatures and densities were in the range $1 \text{ keV} \leq T_e(o) \leq 2 \text{ keV}$ and $2 \times 10^{13} \text{cm}^{-3} \leq n_e(o) \leq 6 \times 10^{13} \text{ cm}^{-3}$.

In Fig. 1 we show measured central plasma velocities in PLT as a function of neutral beam momentum input for deuterium beams into a hydrogen plasma ($D^o + H^+$). The plasma current was 450 kA and the toroidal field 25 kG. The line average electron density, $\bar{n}_e$, ranged over $(2.5 - 3) \times 10^{13} \text{ cm}^{-3}$, and the central electron temperature, which did not change significantly during

injection, was 1.3 ~ 1.5 keV. An essentially linear increase in central toroidal velocity versus momentum input was observed up to values corresponding to neutral beam power $P_b \approx 1$ MW (with particle energy $E_b \approx 40$ keV). The accuracy of measurement of the central velocity lies in the range $\pm$ (1.0 - 1.5) x 10^6 cm/sec.

The maximum central toroidal rotation speed attained, $v_\phi(o) \approx 10^7$ cm/sec, corresponds to ~ 1/6 of the central ion thermal velocity in these experiments. Assuming that rotation damping time scales as a^2, we would expect a rotation speed of 10^8 cm/sec in an 85 cm TFTR plasma with 32 MW of undirectional tangential injection (see insert in Fig. 1). This is comparable to the ion thermal velocity of a 10 keV plasma, and thus could possibly drive Kelvin-Helmholtz instabilities [9].

The dependence of the central toroidal velocity on electron density is shown in Fig. 2 for two beam and plasma species. The beam power is $P_b \approx 1$ MW and the central electron temperature is $T_e(o) \approx 1.1 - 1.3$ keV. We see that higher toroidal velocity results from larger momentum input (D° beams) and smaller plasma mass (lower $\bar{n}_e$, H^+ plasma). The velocity ratio, however, for $D^\circ \rightarrow H^+$ versus $H^\circ \rightarrow D^+$ is not, at constant density, in agreement with the ratio of momentum input to plasma mass, implying a larger momentum confinement time τ_ϕ for D^+ plasmas. In addition, the decrease in plasma rotation with increasing density is less rapid than $1/\bar{n}_e$, implying an increase of τ_ϕ with density.

A series of toroidal plasma rotation measurements were made for a comparison of the velocity induced by co- versus counter-injection. The electron temperature and density were similar for all of these measurements. Electron heating was held to relatively small increases by the density increase associated with beam injection at low electron densities ($\bar{n}_e = 2 \times 10^{13}$ cm^{-3}). The plasma limiter was carbon at a radius of 40 cm. The central

plasma velocities obtained from the use of one co-beam and one counter-beam are shown in Fig. 3 where the different symbols denote different discharges but with the same plasma conditions. The measured velocities occur at varying times as the rotation of the scanning mirrors was not synchronized with the discharge initiation. While the two beam energies are rather close (38 - 40 keV), the power differs significantly, the co-beam power is ~ 400 kW, whereas the counter-beam power is ~ 500 kW. When normalized to constant power, the net induced rotational velocities for co versus counter are identical within our experimental accuracy. Prior to the neutral beam pulse, a central rotation velocity of ~ 1.5 x 10^6 cm/sec in the counter direction is seen, which although of the same magnitude as the experimental accuracy, appears consistently throughout the data. Our failure to observe this small non-beam induced rotation in earlier experiments [8] is due only to a failure to study the non-injection data closely.

Figure 4 shows the results of two simultaneous beams, one co- and one counter-, again at about the same beam energy, 39 - 40 keV, but with co-beam power ≈ 380 kW and a counter-beam power of ≈ 520 kW. Within the accuracy of our measurements, it appears that induced rotation by co + counter-injection is equal to the difference in rotations induced by the beams separately.

Figure 5 gives the central velocity achieved with 2 co-beams delivering ≈ 700 kW total at 34 and 39 keV. The velocity per unit momentum is about 20 percent lower than that deduced from Fig. 3, but this magnitude of scatter is about that expected from the measurement accuracy on a shot-to-shot basis. Certainly toroidal rotation induced by hydrogen beams would be expected to show linearity with input momentum as seen in Fig. 1 with deuterium beams.

Near the plasma periphery, the toroidal velocity was deduced from the Doppler shift of the CV 2271Å line. The radial distribution of this line in relation to the FeXX 2665Å line is shown in Fig. 6 [7]. Ions of CV have a maximum density at a radius r ≈ 30 cm, and a significant concentration in the region between r = 25 to 35 cm. Practically the same radial profiles are obtained with and without neutral beam injection. The FeXX ion distribution becomes peaked at the plasma axis during neutral beam injection into relatively low central electron temperature discharges. This may be a result of charge-exchange recombination [10] with injected hydrogen lowering the ionization balance of iron ions. Before and after injection, FeXX has very similar profiles with a maximum density at r ≈ 8 - 10 cm.

Toroidal velocities deduced from measurements of CV for co- and counter-injections are shown in Fig. 7. Here, as in Fig. 3, the energies of beam particles are approximately the same but the beam powers are ≈ 380 kW and ≈ 520 kW for co- and counter- respectively. Before injection, the velocity at plasma periphery is now seen to be in the co-direction at about 10^6 cm/sec. Again, the velocities, per unit momentum, are symmetric about the initial value. Using two simultaneous co-beams totaling 750 kW produces nearly twice the velocity (Fig. 8) obtained from the single co-beam of Fig. 7.

All of the velocity measurements presented in Figs. 3-5, 7-8 and 9 were made with 0.5 percent (or less) peak-to-peak field ripple on the magnetic axis. Figures 1, 2, and 11, however, were obtained with a single 2.5 percent magnetic well on axis. There is no clearly discernible influence of this perturbation on toroidal rotation. In fact, our efforts to determine energy confinement effects as well as rotation damping attributable to this (2.5 percent) magnetic ripple have produced only null results. While correlations with theory [5,6] is hampered due to the absence of periodicity in the ripple,

this experiment suggests that ripple effects upon rotation may be less sensitive than previously thought [6].

III. MODELING

In order to model the confinement and transport of momentum in these discharges, we need first to calculate the source rate of momentum from the beam particles to the thermal plasma. The Monte Carlo beam-orbit code developed to describe neutral beam heating [11] has been extended to calculate also the momentum input to the background plasma from the beam ions. Momentum is collisionally transferred to the bulk plasma through drag, pitch angle scattering, and energy diffusion, while the radial inward (outward) motion of co- (counter-) injected ions during their thermalization constitutes a $J_r \times B_\theta$ force on the beam ion distribution, slowing down its rotation. The plasma experiences the reaction force through its own radial shielding current.

A major uncertainty in these calculations is the assumed neutral density profile. Ion power balance calculations for neutral beam heating in PLT, assuming neoclassical ion thermal conduction, give an estimate of the central neutral density $n_o(0)$ due to recycling from the walls and limiters of about 5×10^7 cm^{-3}. Assuming this central neutral density, we use a Monte Carlo calculation to determine the radial profile of the neutral density, giving us a value of 10^{10} cm^{-3} at the plasma surface. This is consistent with spectroscopic measurements in the edge region on ST tokamak.

In an attempt to deduce a viscosity (or more properly: momentum diffusivity) coefficient χ (r) from the measured toroidal velocity, we numerically solve the diffusion equation for toroidal momentum [12]

$$n_i m_i \frac{\partial v_\phi}{\partial t} = F(r) - \frac{n_i m_i v_\phi(r)}{\tau_\phi(r)} - \frac{1}{r}\frac{\partial}{\partial r} n_i m_i \chi(r) \frac{\partial}{\partial r} v_\phi \ , \qquad (1)$$

where $F(r)$ is the momentum input calculated using the beam-orbit code, and τ_ϕ^o is the classically expected local damping time due to charge-exchange, and $\chi(r)$ is varied on a trial and error basis to give agreement with experimental data. In this model we have made the assumption that the rotation damping is due to cross-field transport, since we find experimentally that the damping time is comparable in magnitude to the particle and energy confinement times. Nothing in our data, however, rules out the possibility of a local damping process which does not involve transport. Classical and neoclassical viscosity are neglected because they are too small by two orders of magnitude [12,13] to explain the experimental results, and rotation damping due to toroidal field inhomogeneity has been neglected as well. In the absence of the 2.5% local well, theoretical calculations indicate that the field ripple effect is very small, and experimental results show no significant effect from the addition of the 2.5% magnetic well. τ_ϕ^o is given by

$$\left(\tau_\phi^o\right)^{-1} = n_o \langle \sigma v \rangle_{cx} \frac{v_{\phi i} - v_{\phi o}}{v_{\phi i}} \ . \qquad (2)$$

The toroidal rotation velocity of the neutral hydrogen, $v_{\phi o}$, is not locally measured in the core of the plasma, so we have made the reasonable assumption that:

$$v_{\phi o}/v_{\phi i} = T_o/T_i \ ,$$

where T_o is calculated by the neutral transport code. The rotation damping time due to charge-exchange in the center of the plasma is found to be at least an order of magnitude longer than the experimentally determined damping time. However, at the plasma edge the neutral density is high, and the charge exchange damping time can be less than a millisecond.

Our experimental data showing that plasma rotation is proportional to momentum input (Fig. 1), and equally responsive to co- and counter-injection (Fig. 3,7) suggest strongly that the damping mechanism can be modeled as a frictional force or perpendicular viscosity, where the rate of momentum loss from the plasma is proportional to the rotation speed. We see no evidence, for example, of a saturation mechanism occurring at the higher momentum inputs. In order to verify this picture further, it is desirable to model the rise and fall in the plasma rotation, as well as the steady-state profile. For this purpose, the time dependent version of Eq. (2) has been solved using a momentum input of the form

$$F(r,t) = F(r)\ [1 - \exp(-t/\tau_r)] \quad , \tag{3}$$

and τ_r is crudely estimated from

$$\tau_r = N_b m_b v_b / F_{in} \quad ,$$

where $N_b m_b v_b$ is the calculated total beam momentum stored in the plasma, and

F_{in} is the input force from the injector. The τ_r is typically 10-30 msec, and the rise time of the injector power is ~ 15 msec. The total effective rise time of the momentum source is thus ~ 25 msec, a significant fraction of the rise time of the plasma rotation velocity.

Using the model described above we have studied six different injection cases for which we have complete TV Thomson scattering data [14]. The modeling results for a case of co-injection of deuterium beams into a hydrogen plasma [Ref. 8] are shown in Figs. 9a and 9b [examples of $T_e(r)$ and $n_e(r)$ used in the modeling are shown in Figs. 10a and 10b]. In this case the steady-state rotation profile, and the time dependent rise and fall were all described by taking a model for χ similar to the "INTOR" model for electron thermal diffusivity,

$$\chi = 4.5 \times 10^{17}/n_e \ . \qquad (4)$$

The modeling for two further cases of deuterium injection is shown in Fig. 11. Again we find that the rise and fall rates are consistent with the equilibrium rotation speed. In the higher density case the model for χ given in Eq. (4) gave the fit to the data that is shown. In the lower density case, however, the measured rotation speed was quite broad. In the modeling it was necessary to use a viscosity which fell from 6×10^4 at the plasma center to 3×10^4 cm^2/sec at the edge in order to fit the data.

In general, while the radial profile of the anomalous viscosity required to fit the data was not consistent, the magnitude of the viscosity was comparable to the observed electron thermal diffusivity, typically in the range $(1\text{-}5) \times 10^4$ cm^2/sec. The momentum confinement time, which ranged from 10 to 30 msec in the cases studied, was therefore also comparable to the

electron energy containment time, and shorter than the ion energy confinement time deduced for neutral beam heated PLT discharges [11]. A pattern of increasing confinement time with increasing plasma density was observed. For example, for D° injection into H^+ plasma, central momentum confinement time was $\tau_\phi(0) \approx 9$ ms and $\tau_\phi(0) \approx 17$ ms, respectively, for electron density $\bar{n}_e \approx 1.5 \times 10^{13}$ cm^{-3} and 2.8×10^{13} cm^{-3}. This confinement time for H° injection into D^+ plasma was found to be longer, $\tau_\phi(0) \approx 14$ ms and $\tau_\phi(0) \approx 25$ ms, respectively, for $\bar{n}_e \approx 1.6 \times 10^{13}$ cm^{-3} and 3.2×10^{13} cm^{-3}. However, the data is inadequate to give a power law or proportionality constant for the dependence.

Plasma rotation can also in principle be connected with radial electric fields. The relation between the electric field and velocity depends on the contribution of the density and temperature gradients to the plasma rotation. If the neoclassical approach to this problem is correct, in the absence of neutral beam injection one can use a formula by Hazeltine [15] and Hinton and Hazeltine [16] to estimate the radial electric fields in the plasma on the basis of measured toroidal plasma rotation, in a manner similar to Bell [17]. We present below estimates of the radial electric field in PLT based upon neoclassical theory although, clearly, the large deviation of the observed viscosity from the neoclassical value renders such calculations, at best, rough approximations.

Ohmically heated plasmas in PLT are generally in the so-called plateau regime. According to Hinton and Hazeltine [16] and Tsang and Frieman [5], gradients of density, temperature, and electric potential drive the plasma with a toroidal velocity $v_\phi(r)$ given by

$$v_\phi(r) \approx v_\parallel(r) = -\frac{T_i}{eB}\frac{R}{r}q\left[\frac{1}{n_e}\frac{\partial n_e}{\partial r} + [1-(\beta_1, g_{2i})]\frac{1}{T_i}\frac{\partial T_i}{\partial r} + \frac{e}{T_i}\frac{\partial \phi}{\partial r}\right] \quad (5)$$

where (β_1, g_{2i}) evaluated for all regimes of collisionality is given in [16], B is the toroidal magnetic field, ϕ is the electric potential, q is the safety factor, and R is the major radius.

With B = 25 kG, we measure the central toroidal velocity to be $v_\phi = -1.5 \times 10^6$ cm/sec in the counter-direction (without injection). At r = 10 cm, $T_i \approx 600$ eV, $1/T_i\ \partial T_i/\partial r \approx 2.5\ m^{-1}$, $1/n_e\ \partial n_e/\partial_r \approx 1.2\ m^{-1}$, and from Eq. (5) we have,

$$E_r = \partial\phi/\partial r \approx -40\ V/cm \ .$$

At the plasma periphery (r = 30 cm), we have $v_\phi = 1 \times 10^6$ cm/sec in the co-direction, $T_i \approx 200$ eV, $1/T_i\ dT_i/dr \approx 8\ m^{-1}$ and $1/n_e\ \partial n_e/\partial r \approx 8\ m^{-1}$, which leads to

$$E_r \approx -10\ V/cm \ .$$

We note that in PLT, the velocities measured in the plasma center and periphery are comparable in value with velocities driven by gradients of density and temperature, whereas in [17] the measured velocity term was very small in comparison with other terms.

Even though we have calculated electric fields at only two points in minor radius, rough integration of the electric field over a reasonable profile gives a central potential of approximately $\phi \approx -1.2$ kV, the magnitude and polarity of which is consistent with the earlier heavy-ion beam probe measurements made on the ST tokamak [18].

A calculation similar to the above, but for the case with neutral beam injection, gives a potential of $\phi \approx +$ (-) 6 kV for co- (counter-) injection of $\sim$ 1 MW. The use of Eq. (5) for a plasma with neutral beam injection, however, is perhaps even more questionable than for an ohmically heated case, due to the additional momentum sources and any additional dissipative processes taking place [19]. We find, nevertheless, when we apply Eq. (5) to a PLT case with neutral beam injection, that, at least in the central region of the plasma, the electric field contributes much more to the measured toroidal rotation than do the density and temperature gradients. Thus the precise form of the neoclassical diamagnetic-like rotation speed is not important, although the intrinsic assumption of negligible poloidal rotation has a strong effect on the calculated E_r. Measurements of the poloidal rotation speed capable of discriminating between pure toroidal rotation and flow along the field lines are, unfortunately, not available. The large calculated potential, despite its uncertainty, invites speculation on possible changes in the radial impurity fluxes in the presence of anomalous transport.

IV. SUMMARY

In summary, the central toroidal rotation velocity increases linearly with neutral beam momentum input within the accuracy of our measurement, for the range of beam power $P_b \leq 1.0$ MW. In the range of electron density $\bar{n}_e \approx (1.5 - 4) \times 10^{13}$ cm^{-3}, the velocity decreases slowly with increasing $\bar{n}_e$ for both deuterium injected into hydrogen plasma ($D^\circ \rightarrow H^+$) and hydrogen injected into deuterium plasma ($H^\circ \rightarrow D^+$). Toroidal velocities attained for $D^\circ + H^+$ are higher than those for $H^\circ \rightarrow D^+$, but only by about 20 percent, rather less than expected from the beam momentum and plasma mass ratios. No difference was observed in plasma rotation with and without 2.5 percent

magnetic ripple. Without neutral beam injection the plasma rotates in the counter-direction at r ≈ 10 cm with a velocity $v_\phi \approx -1.5 \times 10^6$ cm/sec and in the co-direction at the plasma periphery (r ≈ 30 cm) with $v_\phi \approx 1 \times 10^6$ cm/sec.

Modeling of the radial profile and time evolution of the toroidal rotation gives a perpendicular plasma viscosity in the range of $(1\text{-}5) \times 10^4$ cm^2/sec, approximately two orders of magnitude higher than neoclassically predicted. The momentum confinement time was found to increase as the plasma density was increased, although a precise scaling law could not be given. D^+ plasmas with H^0 injection were found to confine momentum somewhat better than H^+ plasmas with D^0 injection.

A radial electric field E_r was calculated from the Hinton and Hazeltine [16] formula (although the validity of the neoclassical approach is questionable) using the measured plasma toroidal rotation. Without neutral beam injection we roughly estimate the central potential at -1.2 kV, whereas with ~ 1 MW neutral beam co- (counter-) injection this potential is calculated to be +(-) 6 kV.

ACKNOWLEDGMENTS

We would like to acknowledge our gratitude to E. Hinnov for his contribution to this paper and valuable comments, to N. Bretz, D. Dimock, D. Johnson, and D. McNeill for providing us with the TV Thomson scattering data, and to J. Hosea, F. Jobes, E. Meservey, J. Strachan, W. Stodiek, and the Neutral Beam Team for their help in the experiments. We are grateful to H. Furth for helpful discussions of the results and their interpretation. We also wish to express our thanks to M. Bell for his interesting discussions related to electric field calculations.

This work was supported by the U.S. Department of Energy Contract No. DE-AC02-76-CHO-3073.

REFERENCES

[1] ISLER, R.C., CRUME, E.C., ARNURIUS, D.E., and MURRAY, L.E., Oak Ridge National Laboratory Report ORNL/TM-7472 (1980).

[2] BOL, K., et al., in Proceedings of the Seventh International Conference on Plasma Physics and Controlled Nuclear Fusion Research, Innsbruck, Austria, 1978. See also GRISHAM, L. et al., (unpublished); SUCKEWER, S., et al., Princeton Plasma Physics Lab. Report PPPL-1768 (1981).

[3] STACEY, W.M., and SIGMAR, D.J., Phys. Fluids 22 (1979) 2000; Nucl. Fusion 19 (1979) 1665.

[4] BURRELL, K.M., OHKAWA, T., and WONG, S.K., General Atomic Co. Report GA-A16082 (1980) (submitted for publication in Phys. Rev. Lett.); also BURRELL, K.M., Phys. Fluids 23 (1980) 1526.

[5] TSANG, K.T. and FRIEMAN, E.A., Phys. Fluids 19 (1976) 747.

[6] BOOZER, A.N., Plasma Physics Lab. Report PPPL-1619 (1980) (to be published in Phys. Fluids).

[7] SUCKEWER, S., HINNOV, E., and SCHIVELL, J., Bull. Am. Phys. Soc. 23 (1978) 697; Princeton Plasma Physics Lab. Report PPPL-1430, March 1978.

[8] SUCKEWER, S., EUBANK, H.P., GOLDSTON, R.J., HINNOV, E., and SAUTHOFF, N.R., Phys. Rev. Lett 43 (1979) 207.

[9] STIX, T.H., Phys. Fluids 16 (1973) 1922.

[10] SUCKEWER, S., HINNOV, E., BITTER, M., HULSE, R., and POST, D., Phys. Rev. A 22 (1980) 725.

[11] EUBANK, H.P., et al., in Proc. of 7th Int. Conf. on Plasma Physics and Controlled Nuclear Fusion Research, Innsbruck, Austria 1978.

[12] BRAGINSKII, S.I., Review of Plasma Physics, Vol. 1 (LEONTOVICH, M.A., Ed.) Consultants Bureau, New York (1965) 205.

[13] ROSENBLUTH, M.N., RUTHERFORD, P.H., TAYLOR, J.B., FRIEMAN, E.A., and KOVRIZHNYKH, L.M., Plasma Physics and Controlled Nuclear Fusion (Proc. 4th Int. Conf. Madison, 1971) Vol. 1, IAEA, Vienna (1971) 495.

[14] BRETZ, N., DIMOCK, D., FOOTE, S., JOHNSON, D., LONG, D., and TOLNAS, E., Applied Optics 17 (1978) 192.

[15] HAZELTINE, R.D., Phys. Fluids 17 (1974) 961.

[16] HINTON, F.L. and HAZELTINE, R.D., Rev. Mod. Phys. 48 (1976) 239.

[17] BELL, M.G., Nuclear Fusion 19 (1979) 33.

[18] JOBES, F.C., and HOSEA, J.C., in Controlled Fusion and Plasma Physics (Proc. 6th Europ. Conf. Moscow, 1973) Vol. 1 (1973) 199.

[19] SIGMAR, D.J., private communication (1981).

FIGURE CAPTIONS

Fig. 1 Central toroidal plasma velocity as measured from Doppler shifts of the FeXX 2665Å line as a function of neutral beam momentum input for deuterium injection into hydrogen plasma. Indicated in the figure is an extrapolation of the PLT results to the TFTR tokamak with neutral beam power $P_b \approx 32$ MW.

Fig. 2 Central toroidal plasma velocity versus electron density $\bar{n}_e$ for deuterium injection into hydrogen plasma ($D^0 \rightarrow H^+$) and hydrogen injection into deuterium plasma ($H^0 \rightarrow D^+$).

Fig. 3 Central toroidal plasma velocities induced by one co-beam ($P_b \approx 400$ MW) and one counter-beam ($P_b \approx 500$ kW) at 400 to 550 ms and velocity without injection ($t \lesssim 400$ ms).

Fig. 4 Central toroidal plasma velocity during co- plus counter-injection at 400 to 550 ms. $P_b \approx 380$ kW and $P_b \approx 520$ kW for co- and counter-beam, respectively.

Fig. 5 Central toroidal plasma velocity before and during two co-beam injection ($P_b \approx 700$ kW).

Fig. 6 Radial distribution of CV 2271Å and FeXX 2665Å line intensities with and without neutral beam injection.

Fig. 7 Peripheral plasma velocities from Doppler shift of CV 2271Å line before and during one co-beam ($P_b \approx 380$ kW) and one counter-beam ($P_b \approx 520$ kW) injection.

Fig. 8 Peripheral plasma velocity for two co-beams ($P_b \approx 750$ kW).

Fig. 9 Modeling of measured radial profile (a) and time evolution (b) of plasma velocity with $\chi = 4.5 \times 10^{17}/n_e$).

Fig. 10 TV Thomson scattering radial profiles of electron temperature (a) and electron density (b) used for velocity modeling in Fig. 9. (Sources of asymmetry of electron density profile are not known, for modeling purposes profile was symmetrized).

Fig. 11 Modeling of radial profile (a) and time evolution (b) of plasma rotation for two densities: $\bar{n}_e \approx 1.8 \times 10^{13}$ cm^{-3} and 2.8×10^{13} cm^{-3}.

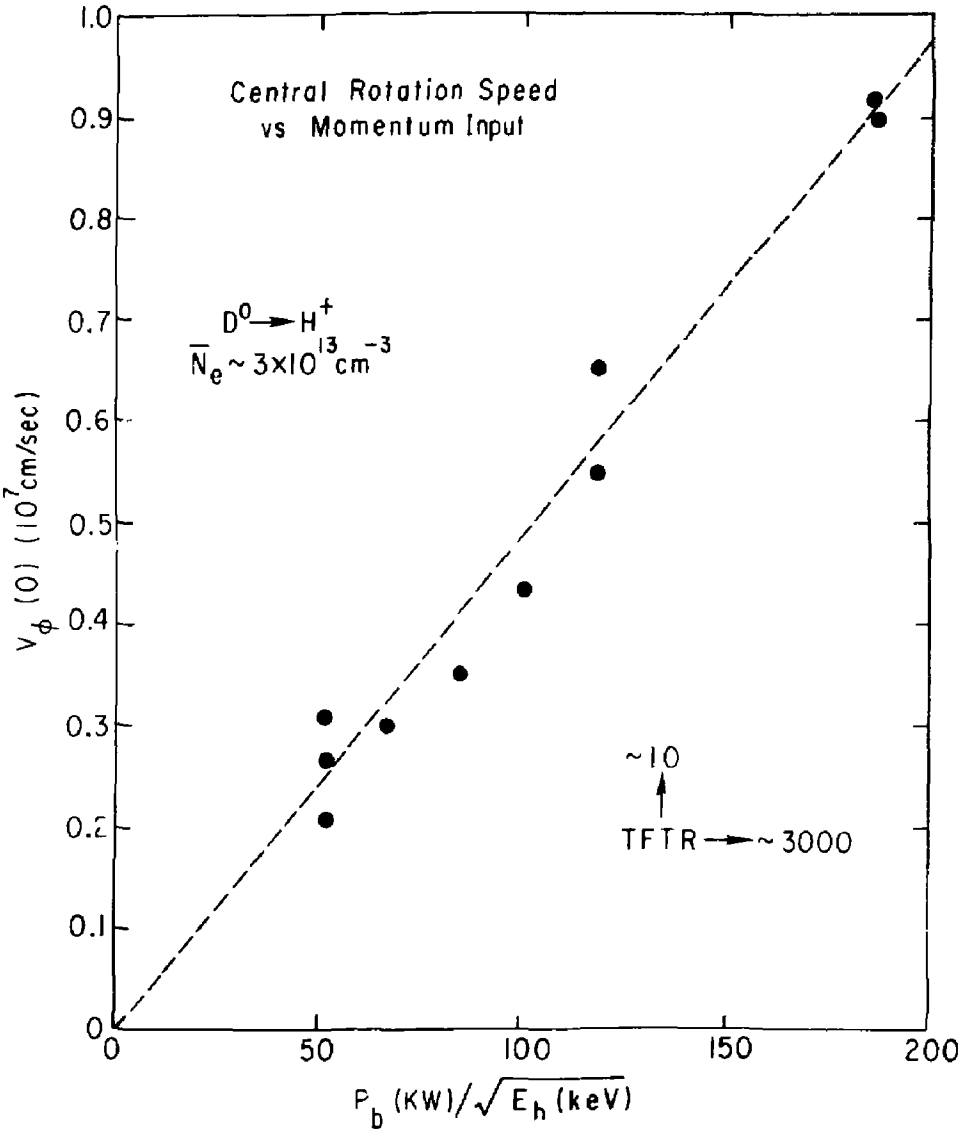

Fig. 1
(PPPL-796384)

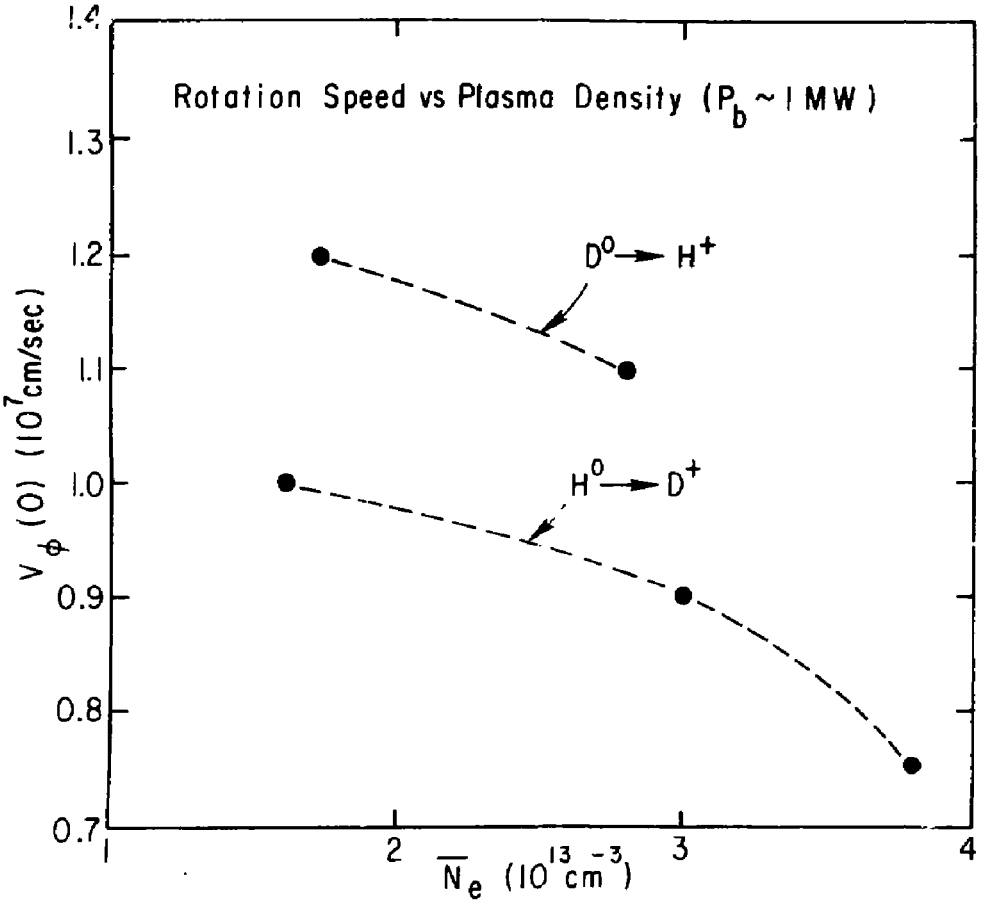

Fig. 2
(PPPL-796383)

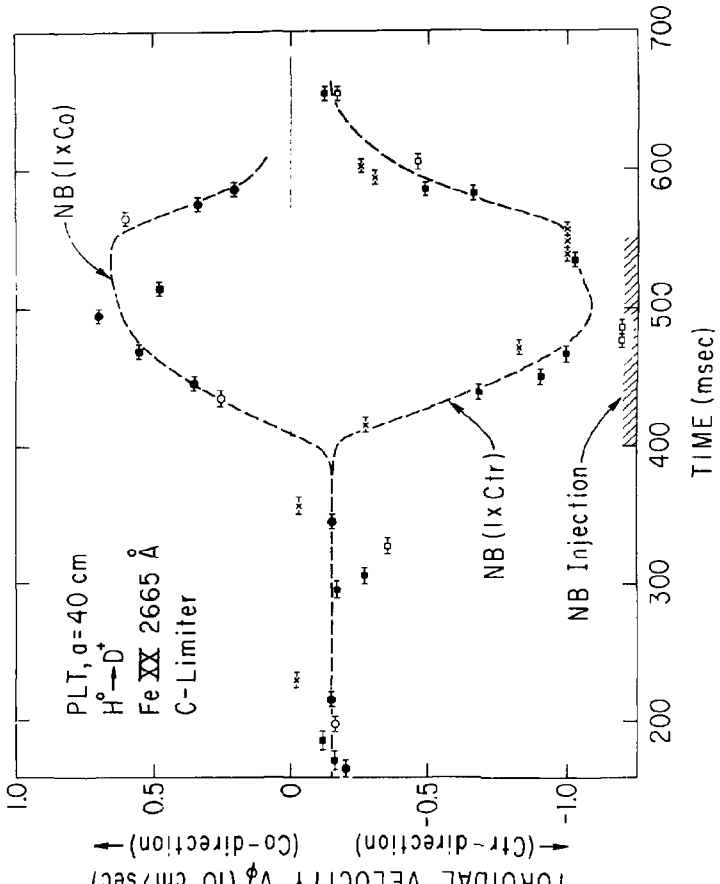

Fig. 3
(PPPL-809132)

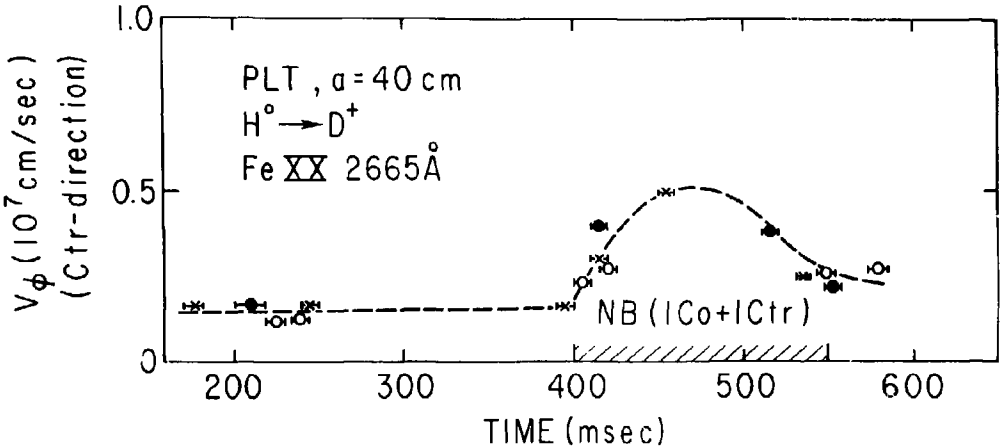

Fig. 4
(PPPL-806166)

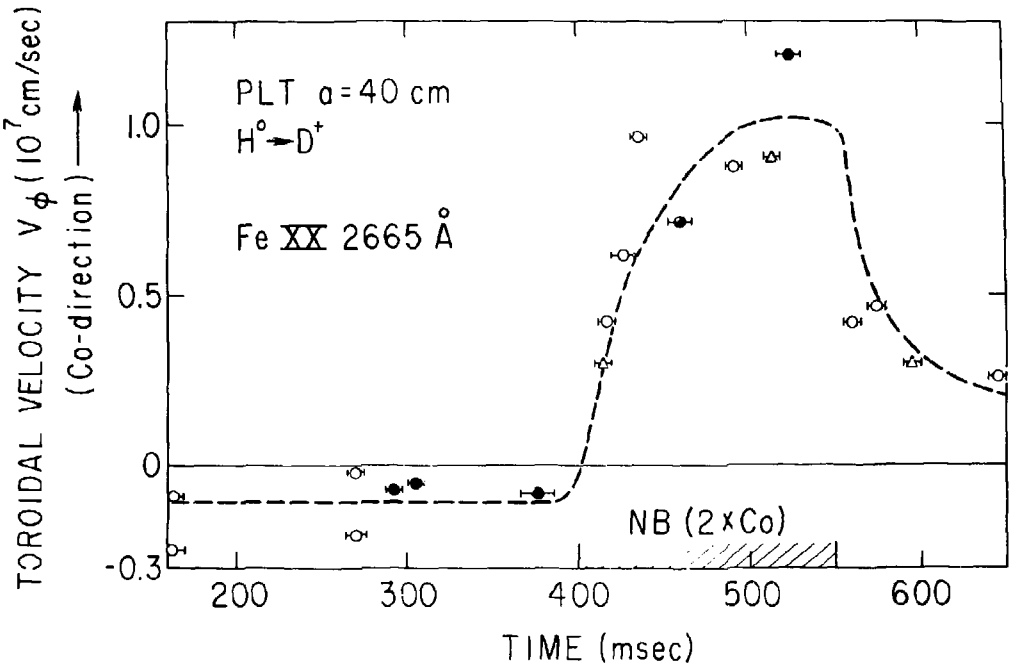
PLT a=40 cm
H°→D⁺
Fe XX 2665 Å
NB (2×Co)
TOROIDAL VELOCITY Vφ (10⁷cm/sec)
(Co-direction)
1.0
0.5
0
-0.3
200
300
400
500
600
TIME (msec)

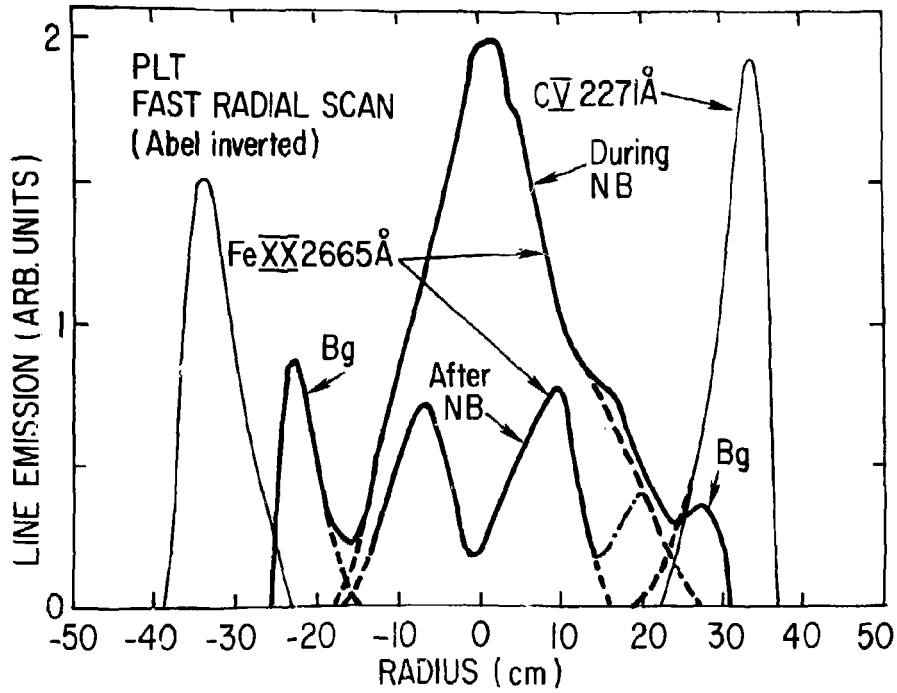

Fig. 6
(PPPL-730569)

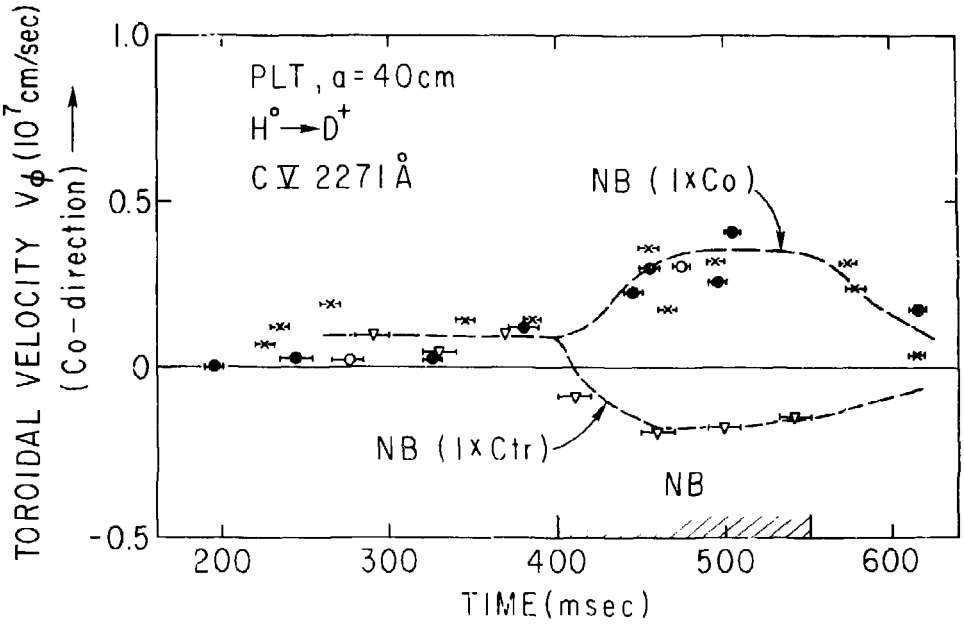
TOROIDAL VELOCITY V_ϕ (10^7cm/sec)
(Co-direction)
1.0
0.5
0
-0.5
PLT, a=40cm
$H^\circ \rightarrow D^+$
C Ⅴ 2271 Å
NB (1xCo)
NB (1xCtr)
NB
200
300
400
500
600
TIME(msec)

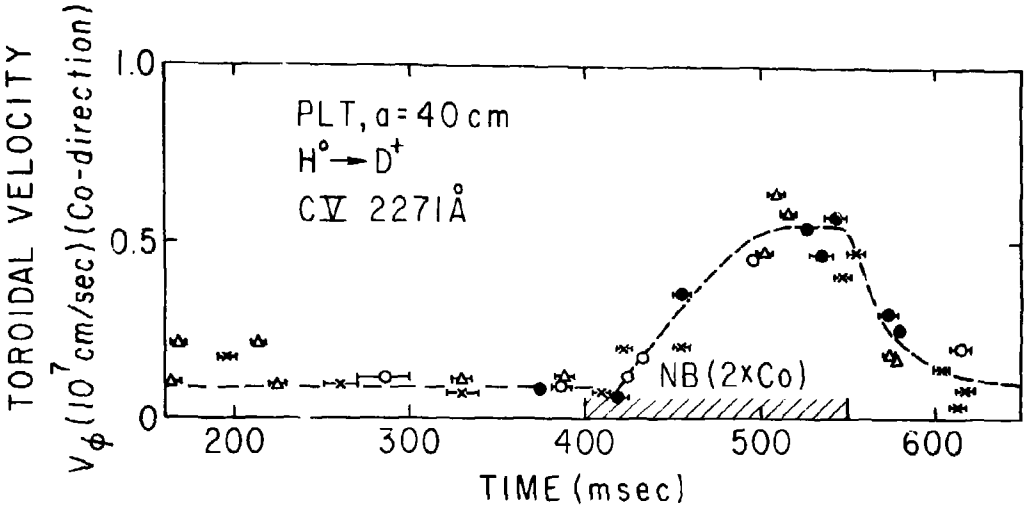

Fig. 8
(PPPL-806[illegible])

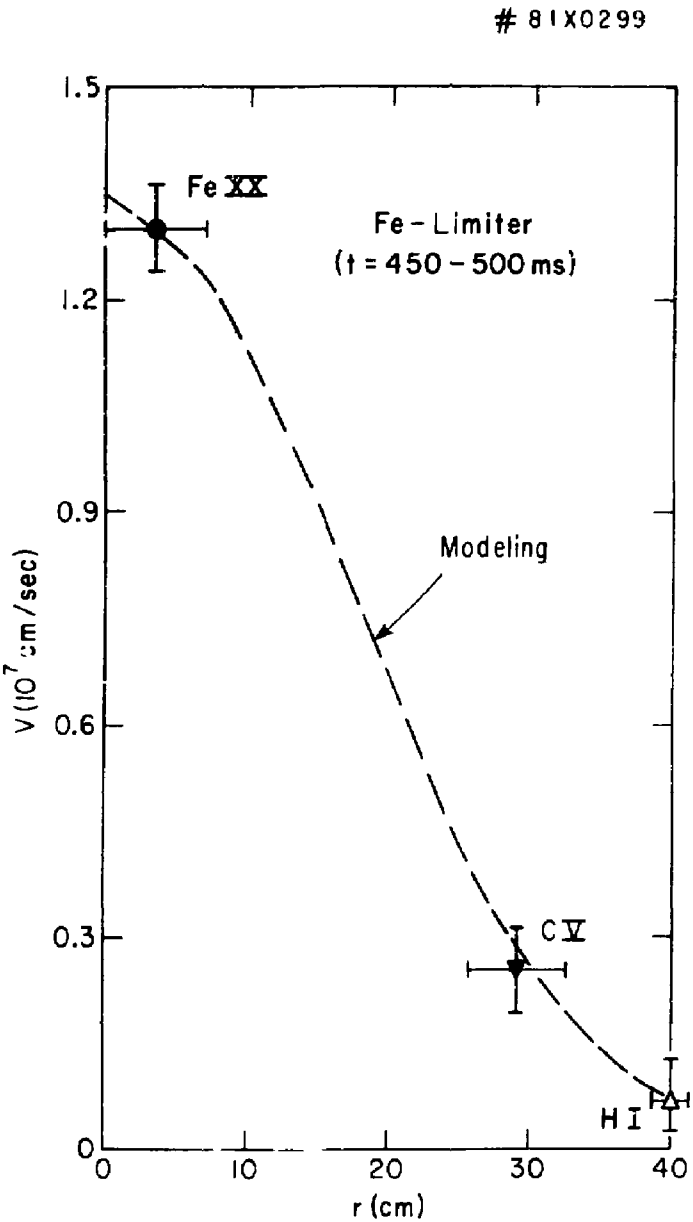
81X0299
1.5
1.2
0.9
0.6
0.3
0
Fe XX
Fe - Limiter
(t = 450 - 500 ms)
Modeling
C V
H I
V (10^7 cm/sec)
0
10
20
30
40
r (cm)

Fig. 9(a)

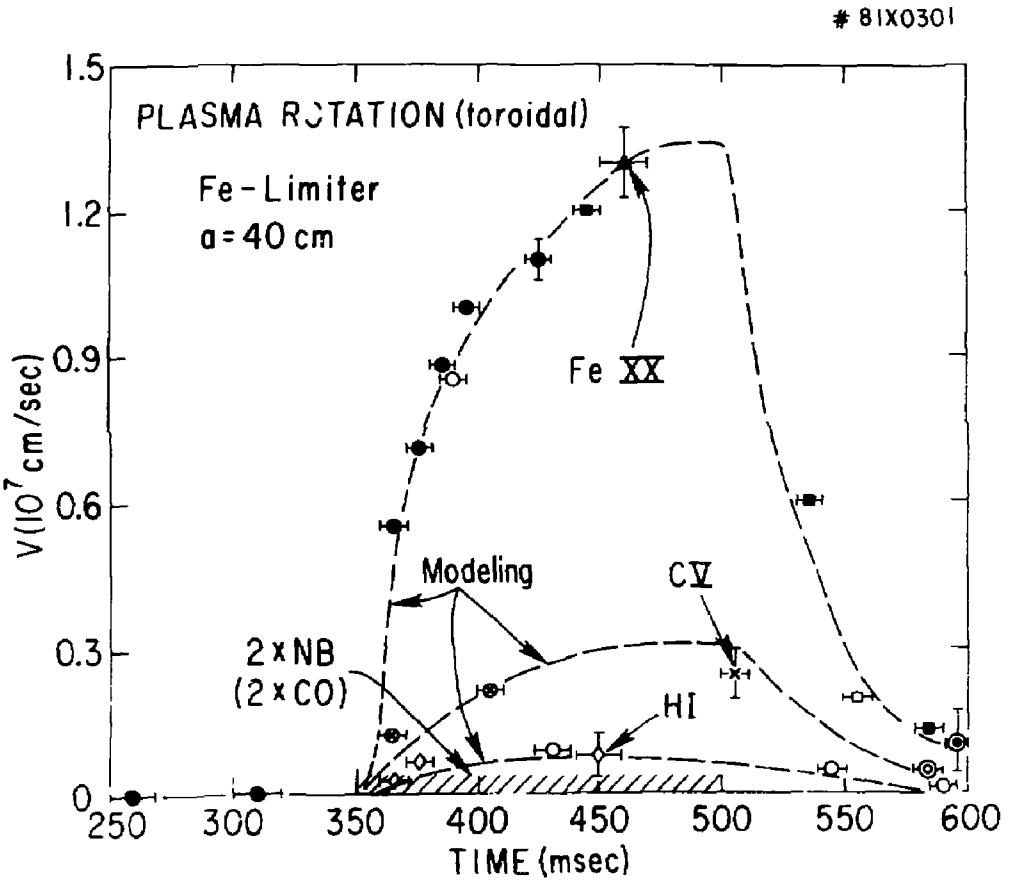
81X0301
PLASMA ROTATION (toroidal)
Fe-Limiter
a=40 cm
Fe XX
Modeling
CV
2xNB
(2xCO)
HI
V(10^7 cm/sec)
TIME (msec)
0
0.3
0.6
0.9
1.2
1.5
250
300
350
400
450
500
550
600

Fig. 9(b)

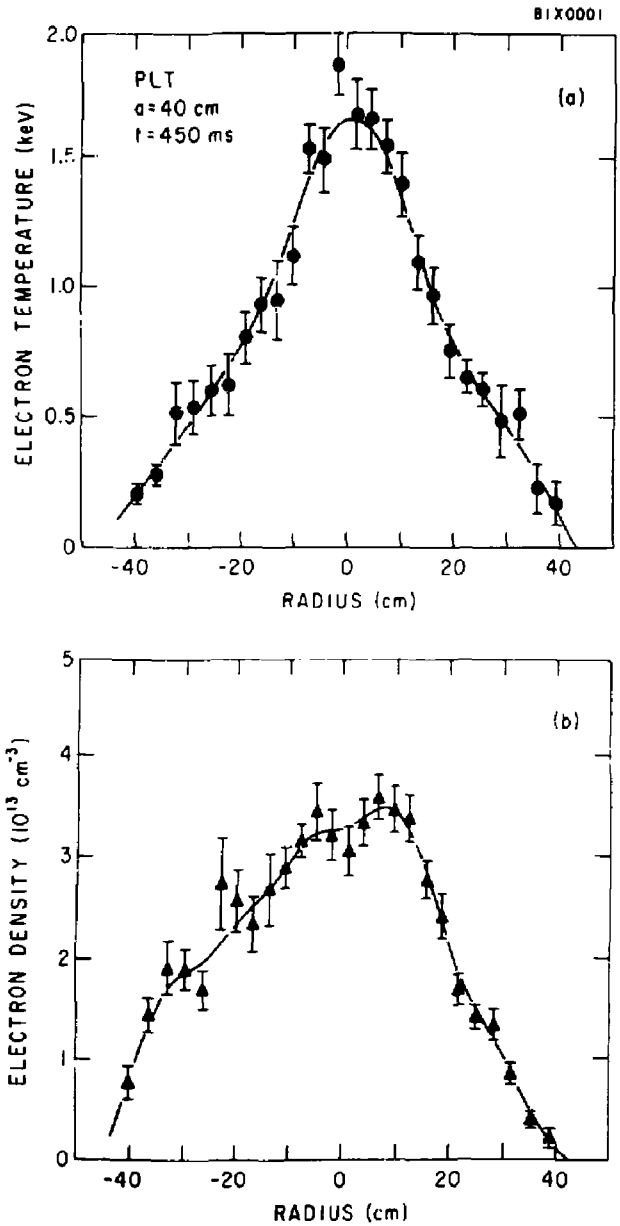
81X0001
PLT
a=40 cm
t=450 ms
(a)
ELECTRON TEMPERATURE (keV)
2.0
1.5
1.0
0.5
0
-40
-20
0
20
40
RADIUS (cm)
(b)
ELECTRON DENSITY (10^{13} cm^{-3})
5
4
3
2
1
0
-40
-20
0
20
40
RADIUS (cm)

Fig. 10 (a) (b)

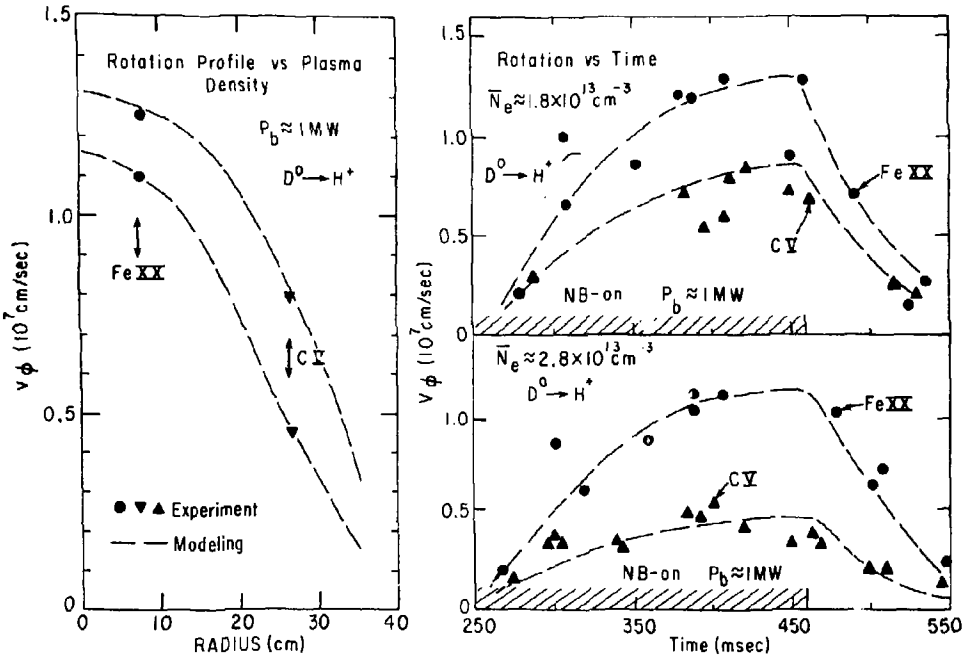
Rotation Profile vs Plasma Density
$P_b \approx 1$MW
$D^0 \rightarrow H^+$
Fe XX
C V
Experiment
Modeling
$v\phi$ (10^7cm/sec)
RADIUS (cm)
Rotation vs Time
$\bar{N}_e \approx 1.8 \times 10^{13}$cm^{-3}
$\bar{N}_e \approx 2.8 \times 10^{13}$cm^{-3}
NB-on $P_b \approx 1$MW
Time (msec)

Fig. 11